Supporting Information for

Large scale production of polyacrylonitrile-based Porous Carbon Nanospheres for Asymmetric Supercapacitors

Yujing Liu[a,b], Jingyi Cao[c], Xiaohui Jiang[a,b], Yange Yang[c,d], Liangmin Yu[a,b]*, Xuefeng Yan [a,b]

[a] *Key Laboratory of Marine Chemistry Theory and Technology, Ministry of Education, Ocean University of China, Qingdao, 266100, China;*

[b] *Qingdao Collaborative Innovation Center of Marine Science and Technology, Ocean University of China, Qingdao, 266100, China;*

[c] *Naval Coatings Analysis and Test Center, Beijing, 102442, China;*

[d] *Laboratory for Corrosion and Protection, Institute of Metal Research, Chinese Academy of Science, Shenyang, 110016, China;*

*Corresponding author E-mail: eproouc@163.com; Tel: (86)-0532-66782533.

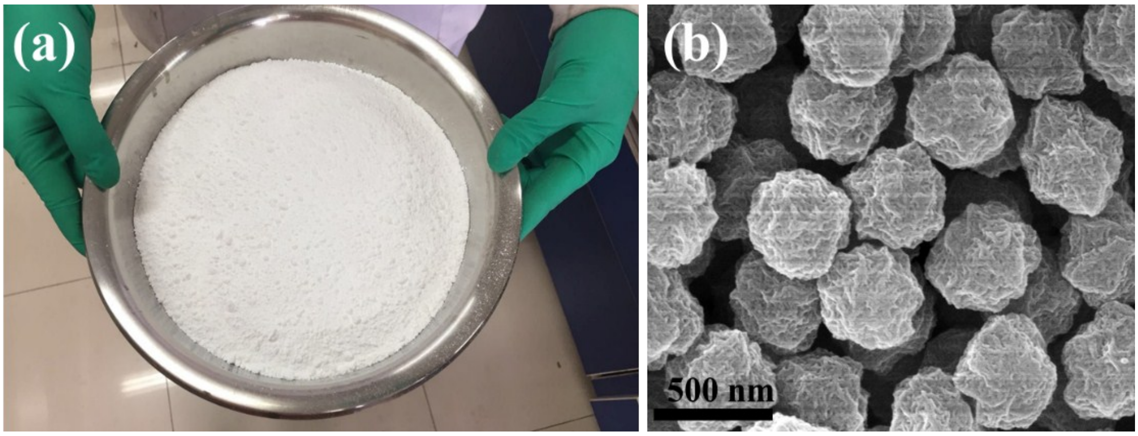

Figure S1 (a, b) Products yielded by 10 L reactor and corresponding SEM image.

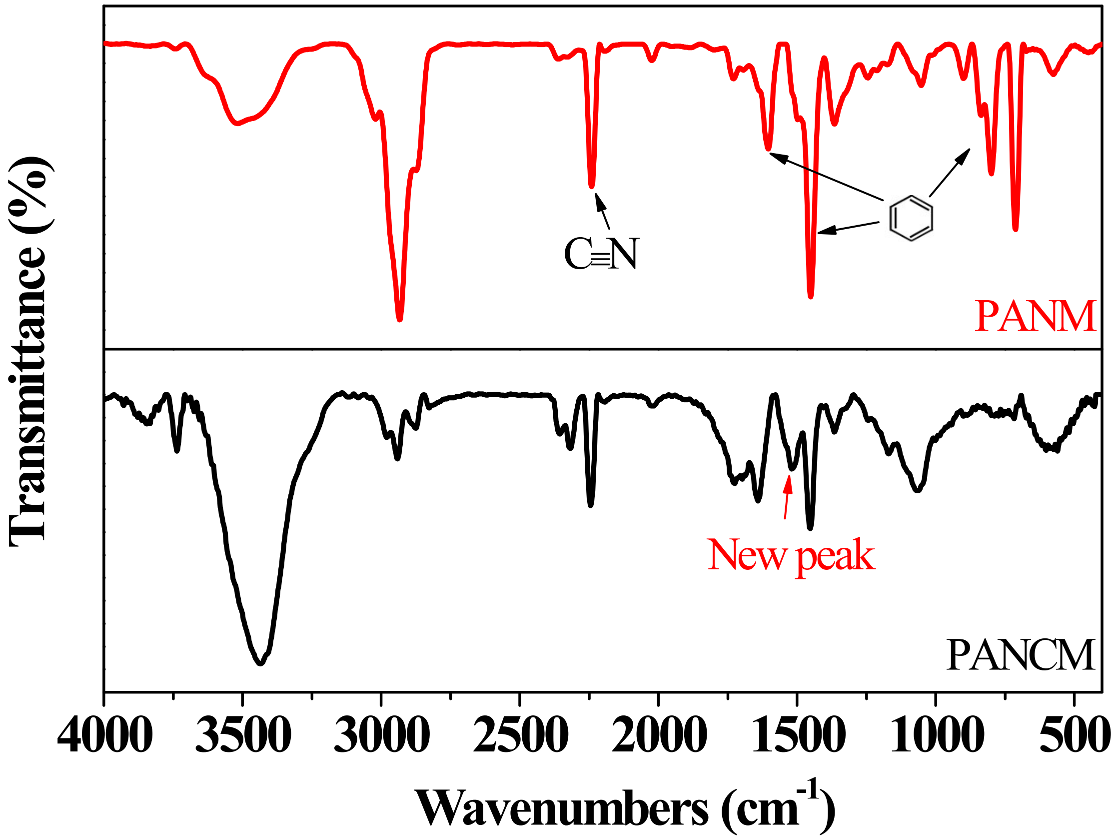

Figure S2 FTIR spectroscopy of PANM and PANCMs.

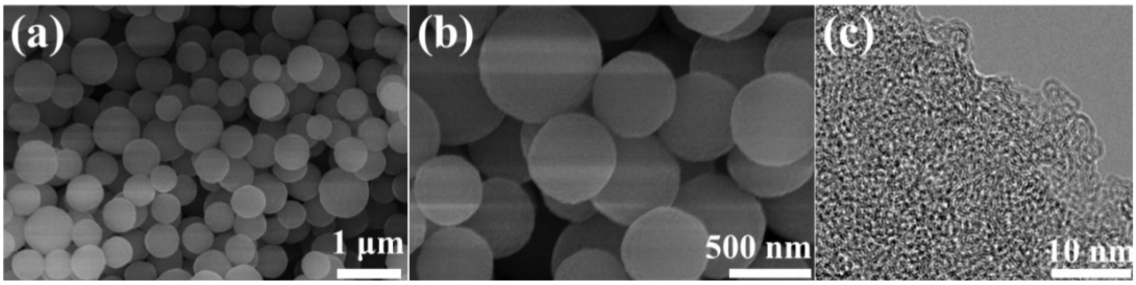

Figure S3 (a, b) SEM images of PAN-wd and (c) HFTEM image of PAN-wd.

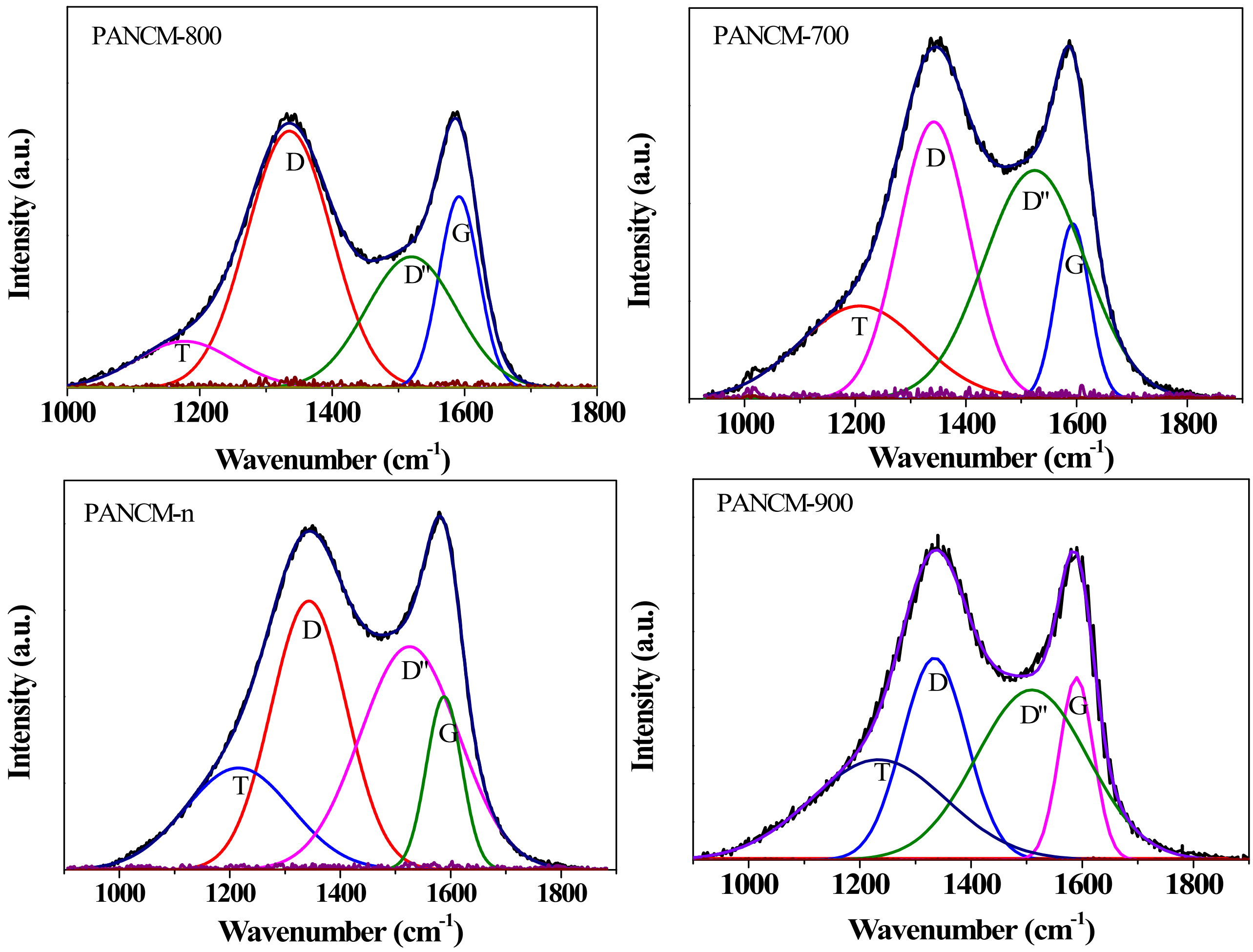

Figure S4 Raman spectra of PANCMs specimens fitted by Voigt function.

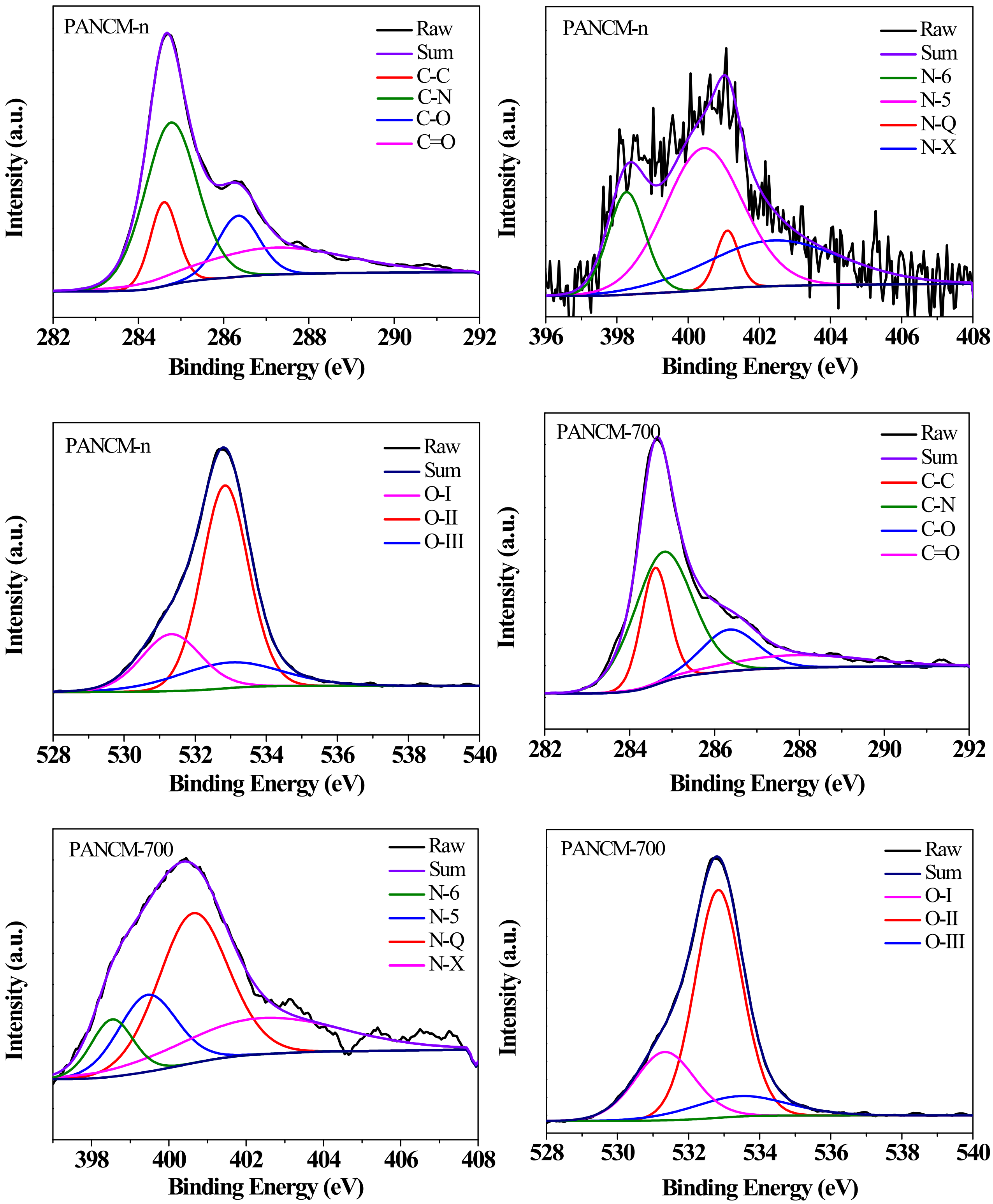
PANCM-n
Raw
Sum
C-C
C-N
C-O
C=O
Intensity (a.u.)
282
284
286
288
290
292
Binding Energy (eV)
PANCM-n
Raw
Sum
N-6
N-5
N-Q
N-X
Intensity (a.u.)
396
398
400
402
404
406
408
Binding Energy (eV)
PANCM-n
Raw
Sum
O-I
O-II
O-III
Intensity (a.u.)
528
530
532
534
536
538
540
Binding Energy (eV)
PANCM-700
Raw
Sum
C-C
C-N
C-O
C=O
Intensity (a.u.)
282
284
286
288
290
292
Binding Energy (eV)
PANCM-700
Raw
Sum
N-6
N-5
N-Q
N-X
Intensity (a.u.)
398
400
402
404
406
408
Binding Energy (eV)
PANCM-700
Raw
Sum
O-I
O-II
O-III
Intensity (a.u.)
528
530
532
534
536
538
540
Binding Energy (eV)

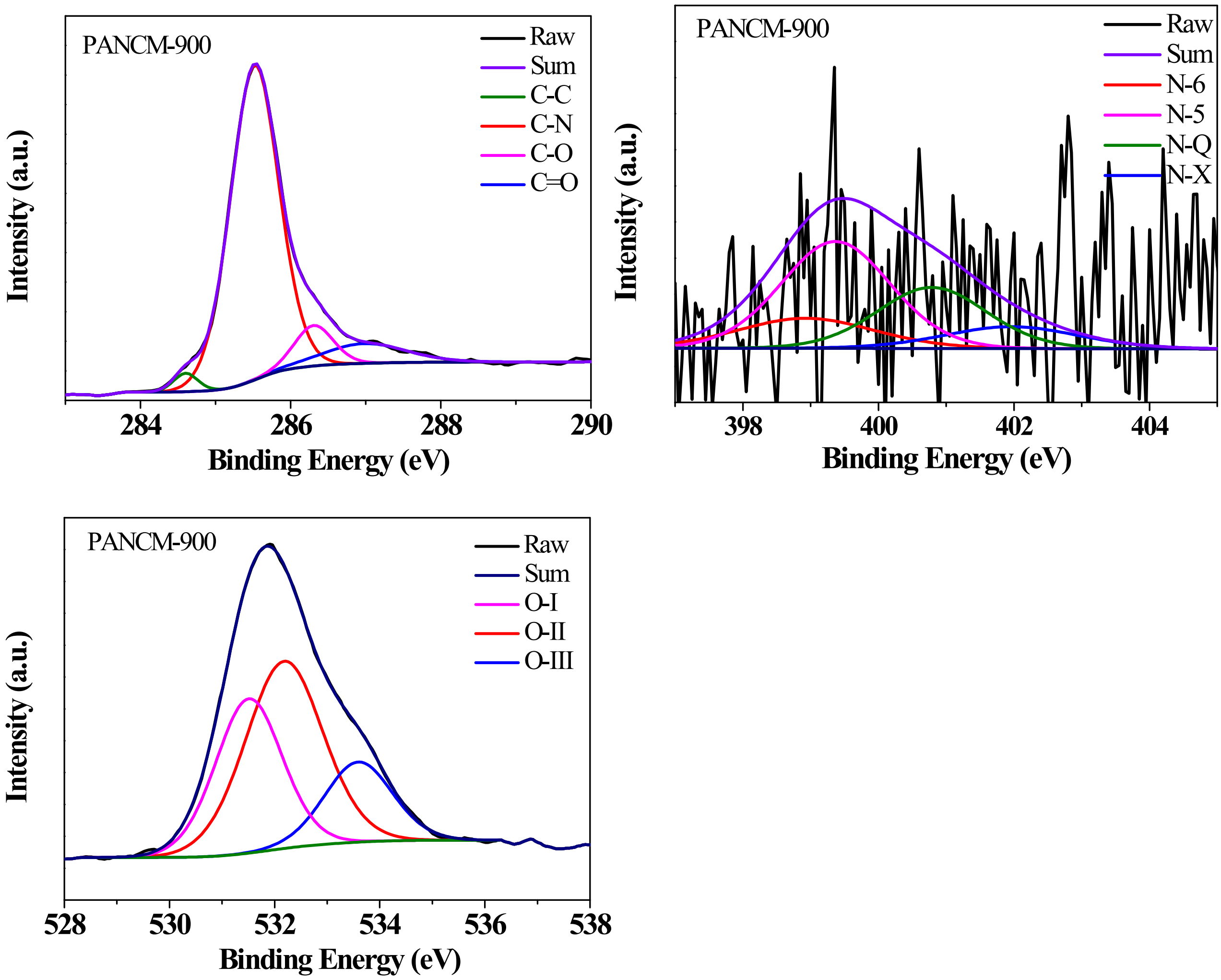

Figure S5 Curve-fitted high-resolution XPS scans of PANCMs for C 1s, N 1s and O 1s.

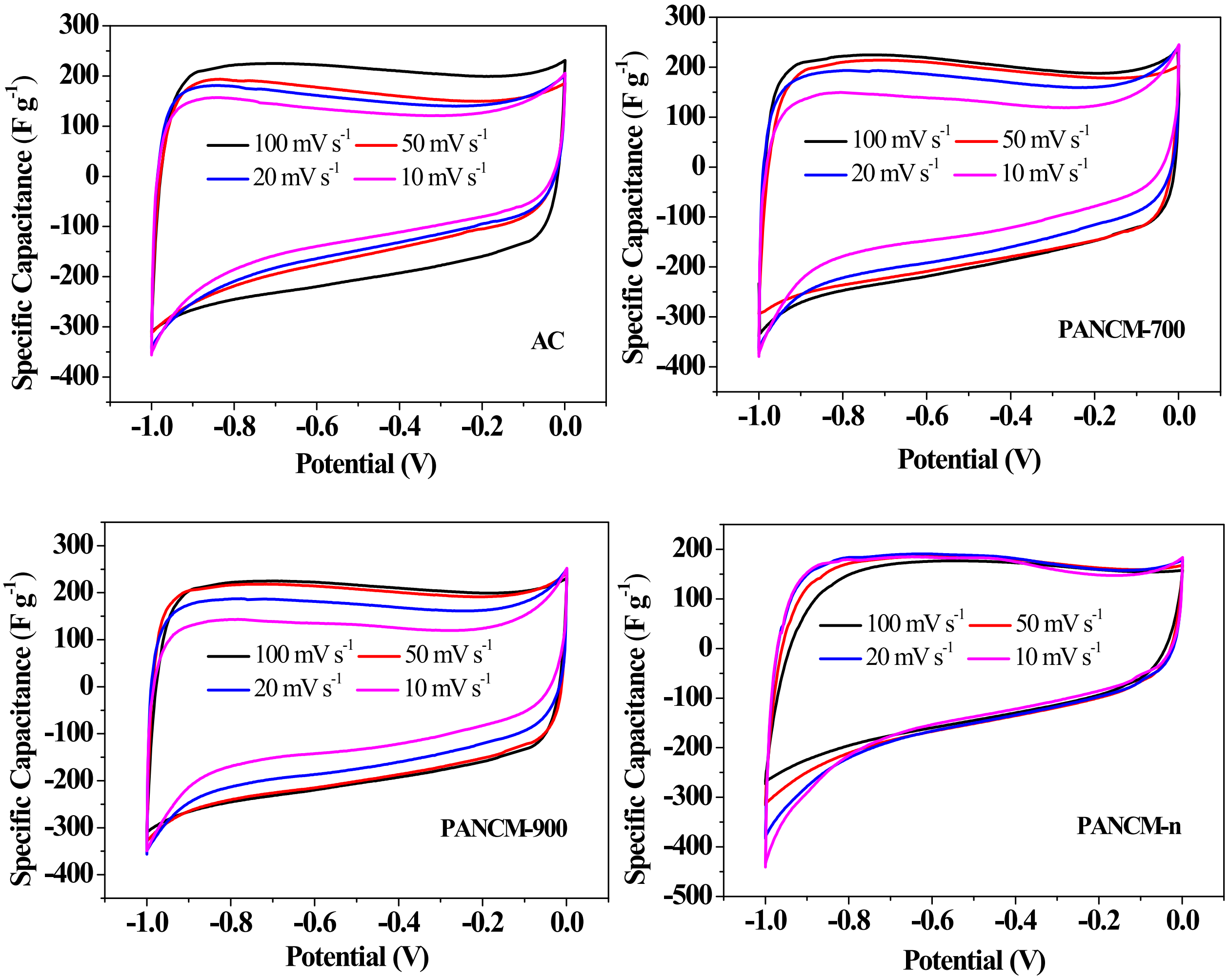

Figure S6 CV curves of AC, PANCM-700, PANCM-900 and PANCM-n at different scan rates.

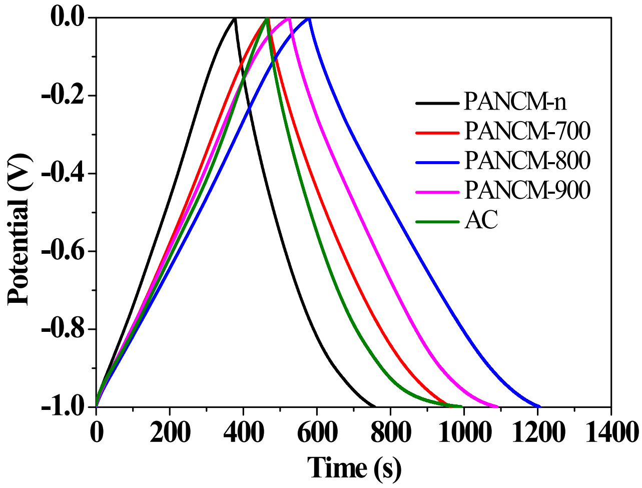

Figure S7 Galvanostatic charge/discharge profiles of PANCMs at 0.5 A g^{-1} under three-electrode system.

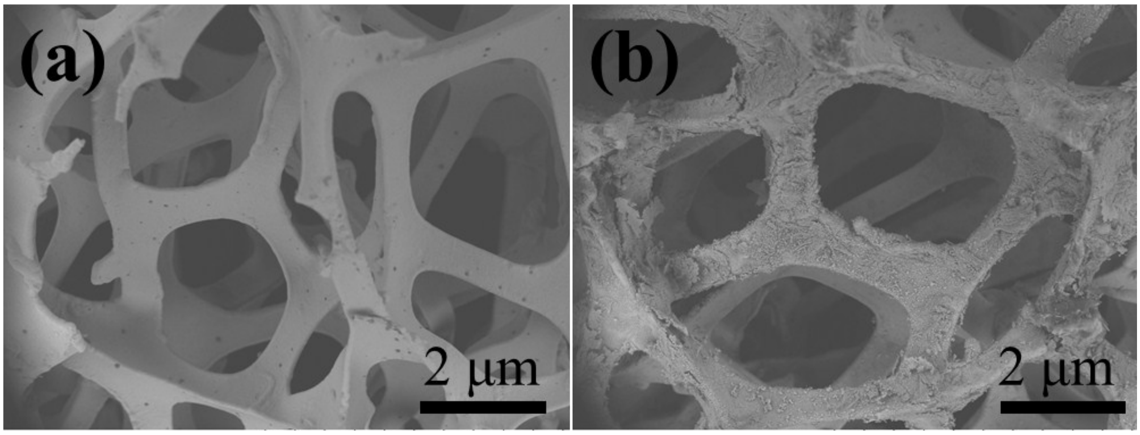

Figure S8 The SEM images of bare Ni foam and Ni foam coated with $Co_{0.9}Mn_{0.1}$ oxide.

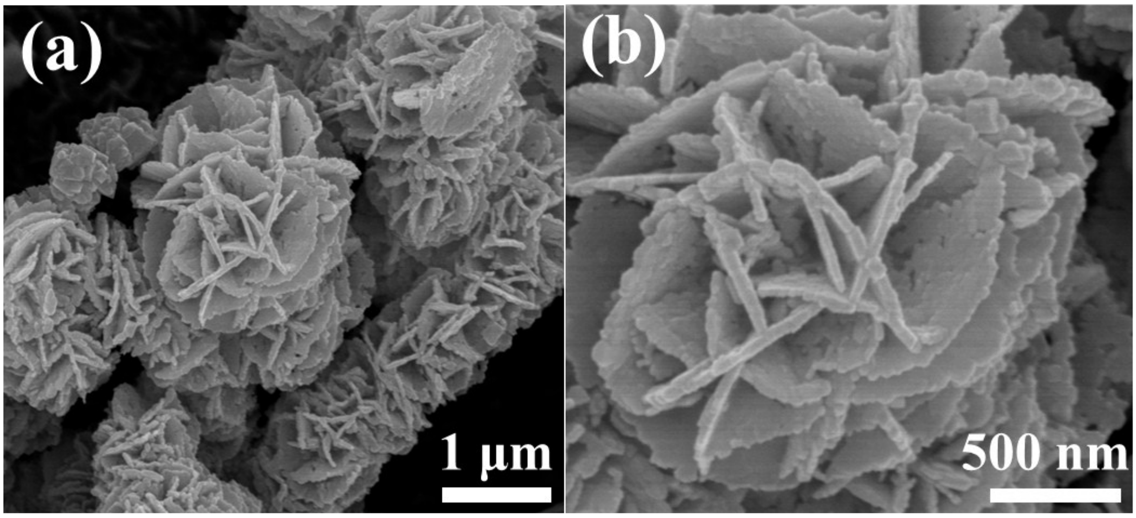

Figure S9 SEM images of $Co_{0.9}Mn_{0.1}$ oxide.

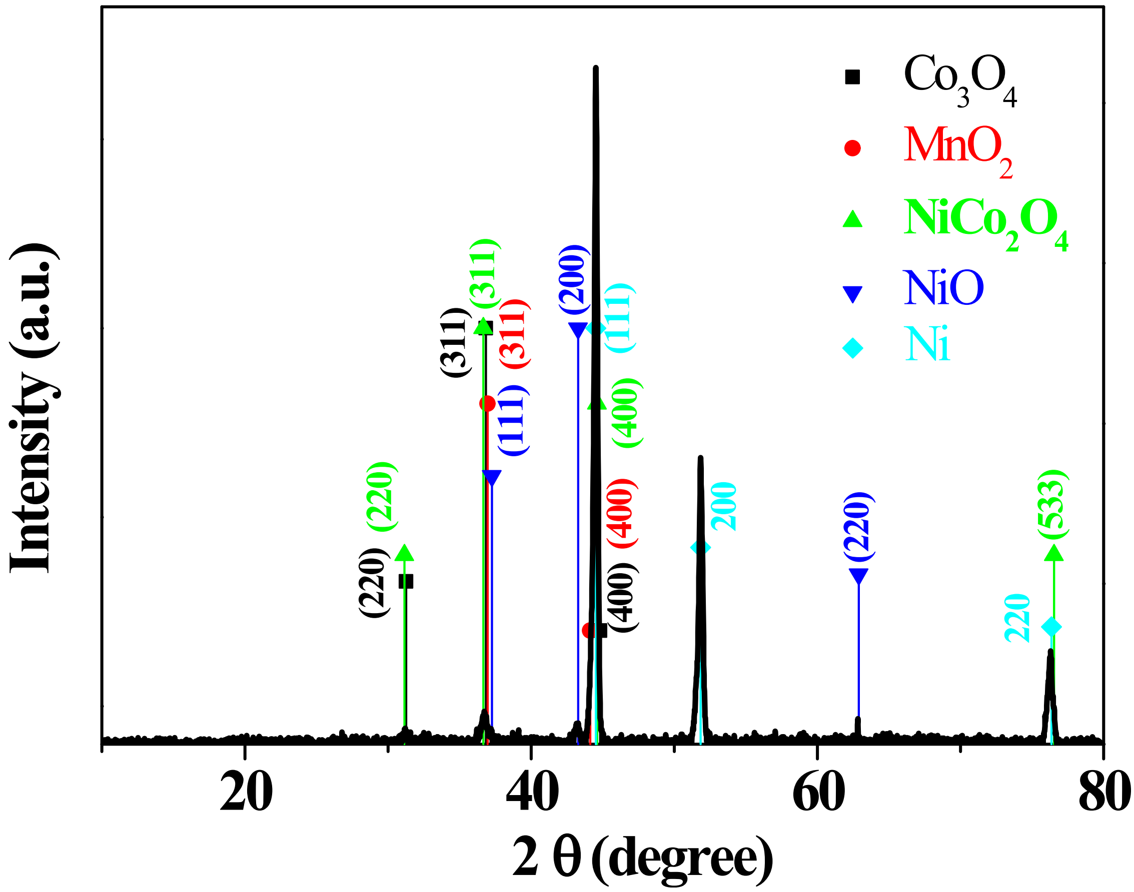

Figure S10 XRD patterns of $Co_{0.9}Mn_{0.1}$ arrays.

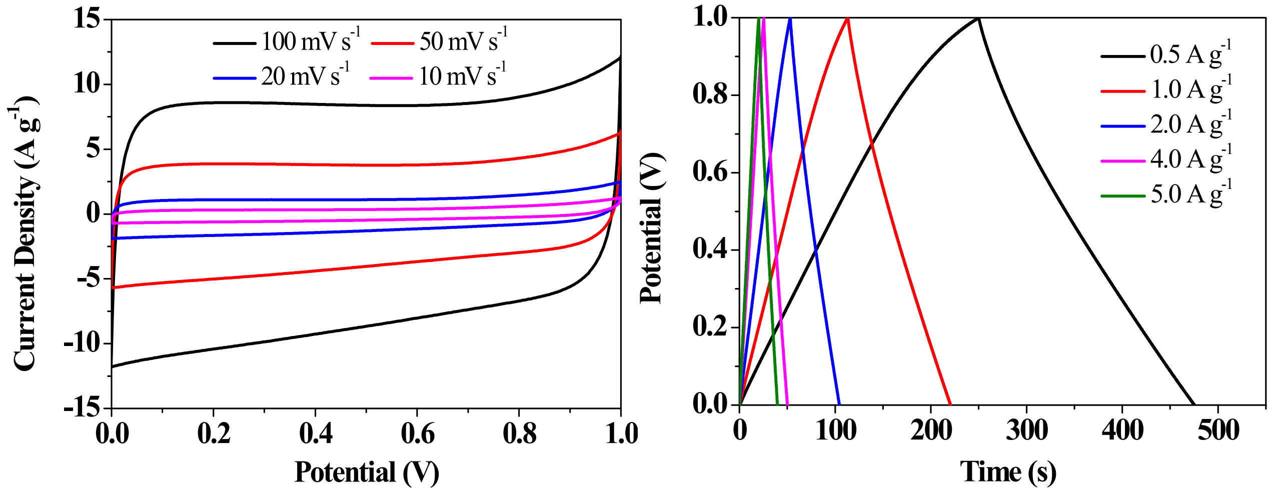

Figure S11 (a) CV plots of PANCM-800//PANCM-800 device and (b) corresponding charge-discharge curves at different current densities.

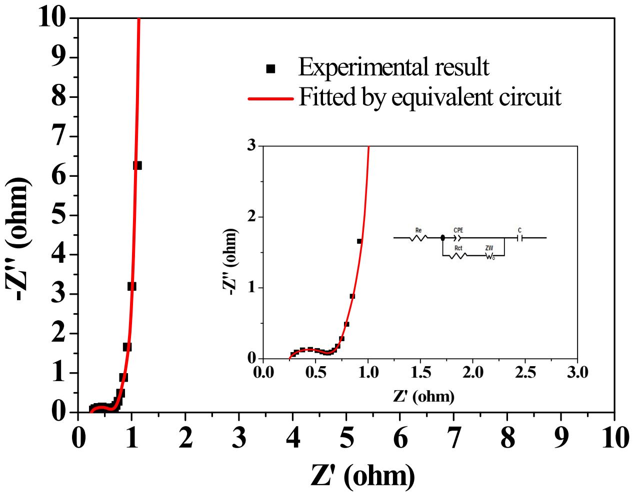

Figure S12 Nyquist plot of PANCM-800//$Co_{0.9}Mn_{0.1}$ device and equivalent circuit model.

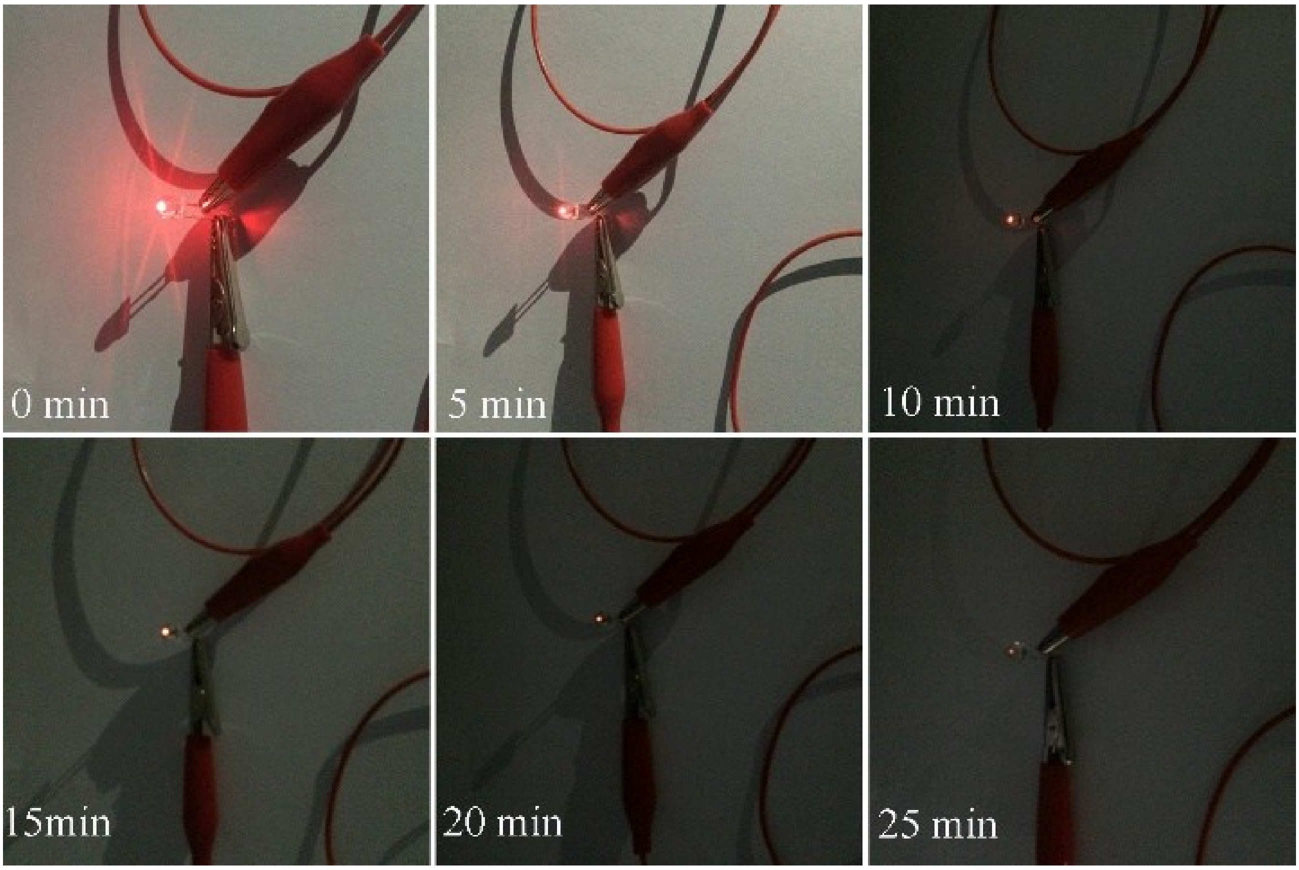

Figure S13 Red LED powered by two devices connected in series.

Table S1 XPS composition (N and O at%) of PANCMs obtained by fitting.

Samples	N-6	N-5	N-Q	N-X	O-1	O-2	O-3
PANCM-n	16.62	50.76	5.17	27.45	21.92	61.06	17.22
PANCM-700	10.33	19.27	44.92	25.48	23.78	78.82	3.40
PANCM-800	10.40	22.31	59.33	7.96	28.78	63.63	7.59
PANCM-900	16.08	46.03	26.31	11.57	33.98	48.02	18.00

Table S2 Parameters of the equivalent circuit and electrical conductivity for different electrodes.

Materials	R_e (Ω)	R_{ct} (Ω)	Z_w (Ω)	conductivity (S/m)
AC	0.236	0.277	0.564	31.0
PANCM-n	0.238	0.572	0.997	2.2
PANCM-700	0.185	0.284	0.251	77.1
PANCM-800	0.191	0.240	0.224	251.2
PANCM-900	0.218	0.243	0.285	260.4

Table S3 Comparison of electrochemical performance of carbon materials derived from PAN.

Materials	**Electrolyte**	**Capacitance ($F g^{-1}$)**		**Cell**	**Capacitance retention (%)/ Rate ($A g^{-1}$)**	**Number. of cycles**	Ref.
		Low rate ($A g^{-1}$)	**High rate ($A g^{-1}$)**				
PASC [a]	2M KOH	185 (0.625)	170 (2)	3E	97.5 (2)	10000	S1
NHPC [b]	6M KOH	257 (0.5)	128 (20)	3E	90.38 (1)	10000	S2
NPC-PAN [c]	1M H_2SO_4	210 (0.1)	189 (1)	2E	-	-	S3
HPCs [d]	6M KOH	314 (0.5)	237 (20)	3E	96 (5)	2000	S4
HPCNs [e]	6M KOH	240 (1)	-	2E	96 (5)	3000	S5
CLCNF [f]	1M H_2SO_4	206 (0.5)	101 (800)	3E	75.3 (10)	1000	S6
PAN [g]	6M KOH	240 (0.05)	168 (50)	2E	92 (1)	5000	S7
	1M H_2SO_4	200 (0.05)	150 (50)	2E	75 (1)	5000	
PMC [h]	1M H_2SO_4	270 (0.2)	195 (100)	3E	100 (20)	5000	S8
NCF [i]	1 M H_2SO_4	242	80	3E	99 (1)	5000	S9

		(0.2)	(5)				
NPC-S [j]	1M Na_2SO_4	244 (0.1)	100 (20)	2E	85 (2)	10000	S10
CNF [k]	2M KOH	210 (2 mV/ s)	49 (200 mV/s)	3E	100 (50 mV s^{-1})	2000	S11
NHPC [l]	2M KOH	314 (0.5)	215 (20)	3E	90 (2)	10000	S12
HPCNFs [m]	2M H_2SO_4	307 (1)	193.4 (50)	2E	98.2 (5)	10000	S13
N-HMSCCs[n]	6M KOH	206 (1)	127 (10)	3E	92.3 (5)	3000	S14
HPC [o]	6M KOH	51 (0.5)	38.25 (32)	2E	96 (5)	50000	S15
NPCNFs [p]	1M H_2SO_4	224.9 (0.5)	155.5 (30)	3E	105.2 (5)	8000	S16
HMCSs [q]	1M H_2SO_4	298.6 (1)	212 (20)	3E	97.3 (1)	5000	S17
PANCNT [r]	1M H_2SO_4	216 (10 mV/s)	150 (50 mV/s)	3E	108 (50 mV s^{-1})	3000	S18
PANCM	2M KOH	290 (0.5)	200 (20)	3E	93 (10)	3000	This work

[a] PAN-b-PS-b-PAN; [b] nitrogen-doped hierarchical carbon; [c] PAN-based nanoporous carbon; [d] beehive-like hierarchical porous carbons; [e] hierarchical porous carbon nanospheres; [f] cross-linked carbon nanofiber; [g] PAN-based nanofiber paper; [h] N-doped porous monolithic carbons; [i] nitrogen-enriched carbon fibers; [j] nanoporous carbon spheres; [k] carbon nanofibers; [l] nitrogen-doped

hierarchical porous carbon; [m] hollow particle-based; [n] nitrogen-doped carbon nanofibers; [o] nitrogen-doped hollow mesoporous spherical carbon capsules; [p] hierarchically porous carbon; [q] nitrogen/phosphorus co-doped nonporous carbon nanofibers; [r] hollow mesoporous carbon spheres.

References

S1 Y. Wang, L.B. Kong, X.M. Li, F. Ran, Y.C. Luo and L. Kang, *New Carbon Materials*, 2015, 30(4), 302-309.

S2 Y.X. Tong, X.M. Li, L.J. Xie, F.Y. Su, J.P. Li, G.H. Sun, Y.D. Gao, N. Zhang, Q. Wei and C.M. Chen, *Energy Storage Materials*, 2016, 3, 140-148.

S3 X.Q. Yang, D.C. Wu, X.M. Chen and R.W. Fu, *J. Phys. Chem. C*, 2010, 114, 8581-8586.

S4 L. Yao, G.Z. Yang, P. Han, Z.H. Tang and J.H. Yang, *J. Power Sources*, 2016, 315, 209-217.

S5 L. Yao, G.Z. Yang and P. Han, *RSC Adv.*, 2016, 6, 43748-43754.

S6 G.B. Xue, J. Zhong, Y.L. Cheng and B. Wang, *Electrochim. Acta*, 2016, 215, 29-35.

S7 E.J. Ra, E. Raymundo-Piñero, Y.H. Lee and F. Béguin, *Carbon*, 2009, 47, 2984-2992.

S8 Y. Shu, J. Maruyama, S. Iwasaki, S. Maruyama, Y.H. Shen and H. Uyama, *RSC Adv.*, 2017, 7, 43172-43180.

S9 L. Fan, L. Yang, X.Y. Ni, J. Han, R. Guo and C.F. Zhang, *Carbon*, 2016, 107, 629-637.

S10 J.N. Zhang, R. Yuan, S. Natesakhawat, Z.Y. Wang, Y.P. Zhao, J.J. Yan, S.Y. Liu, J. Lee, D.L. Luo, E. Gottlieb, T. Kowalewski, M.R. Bockstaller and K. Matyjaszewski, *ACS Appl. Mater. Interfaces.*, 2017, 9, 37804-37812.

S11 C.C. Lai and C.T. Lo, *Electrochimica Acta*, 2015, 183, 85-93.

S12 K. Yan, L.B. Kong, K.W. Shen, Y.H. Dai, M. Shi, B. Hu, Y.C. Luo and L. Kang, *Appl. Surf. Sci.*, 2016, 364, 850-861.

S13 L.F. Chen, Y. Lu, L. Lu and X.W. Lou, *Energy Environ. Sci.*, 2017, 10, 1777-1783.

S14 A.B. Chen, K.C. Xia, L.S. Zhang, Y.F. Yu, Y.T. Li, H.X. Sun, Y.Y Wang, Y.Q. Li and S.H. Li, *Langmuir*, 2016, 32, 8934-8941.

S15 F.J. Miao, C.L. Shao, X.H. Li, K.X. Wang, N. Lu and Y.C. Liu, *J. Mater. Chem. A.*, 2016, 4, 5623-5631

S16 X.D. Yan, Y. Liu, X.R. Fan, X.L. Jia, Y.H. Yu and X.P. Yang, *J. Power Sources.*, 2014, 248, 745-751.

S17 C. Liu, J.Z. Liu, J. Wang, J.S. Li, R. Luo, J.Y. Shen, X.Y. Sun, W.Q. Han and L.J. Wang, J. *Colloid Interface Sci.*, 2018, 512, 713-721.

S18 Y.Q. Wang, B. Fugetsu, Z.P. Wang, W. Gong, I. Sakata, S. Morimoto, Y. Hashimoto, M. Endo, M. Dresselhaus and M. Terrones, *Scientific Reports*, 2017, 7, 40259.